Microelectronic Engineering 178 (2017) 89–92

Contents lists available at ScienceDirect

Microelectronic Engineering

journal homepage: www.elsevier.com/locate/mee

Tuning the conductivity of resistive switching devices for electronic synapses

M. Pedro [a,*], J. Martin-Martinez [a], M.B. Gonzalez [b], R. Rodriguez [a], F. Campabadal [b], M. Nafria [a], Xavier Aymerich [a]

[a] Universitat Autònoma de Barcelona, Dept. Enginyeria Electronica Edifici Q, 08193 Bellaterra, Spain
[b] Institut de Microelectrònica de Barcelona, IMB-CNM, CSIC, Campus UAB, 08193 Bellaterra, Spain

ARTICLE INFO

Article history:
Received 20 February 2017
Received in revised form 26 April 2017
Accepted 27 April 2017
Available online 03 May 2017

Keywords:
Electronic synapse
MIM
Neuromorphic circuits
RRAM
Resistive switching

ABSTRACT

The implementation of electronic synapses is today one of the challenges of hardware-based neuromorphic engineering, which aims to design electronic circuits with a similar architecture and behavior those found in biological brains. In this work, the control of the conductivity of MIM structures was investigated in order to determine their suitability for the implementation of electronic synapses in neuromorphic circuits. Electrical characterization consisting of cyclic voltammetry was carried out under two different schemes, both involving the gradual variation of the compliance current from cycle to cycle. The smart interruption of the measurement in one of the test schemes allowed the study of the conductivity characteristics according to the Quantum Point Contact (QPC) model. Obtained results showed that the conductivity of the tested devices can be tuned by means of gradually modifying the compliance current driving each device.

1. Introduction

The difficulty of overcoming the limitation on throughput caused by the disparity between processors and data access speeds in the standard Von Neumann computer architecture, along with the recent progress in the development of new classes of nanodevices involving resistive switching (RS) phenomena, enabled the emergence of alternative approaches to the Von Neumann model, such as bio-inspired architectures, also referred to as neuromorphic systems. This paradigm parts from the artificial neural networks (ANN) model, which describes the computation performed by the biological brain. ANN are self-learning systems in which the storage and computation units are merged: computing nodes, i.e. neurons, are in charge of integrating the large number of inputs that they receive through weighted connections, i.e. synapses. Biologically, the arrival of an input to a neuron depolarizes it, meaning that the potential difference between its body and the external medium (transmembrane potential) is more significant. When a neuron achieves a certain threshold due to depolarization, it transmits to other post-synaptic neurons through synapses, which are gap junctions where electrical or chemical signaling between two neurons occurs. Whereas the computing nodes have already been successfully implemented with CMOS technology [1–2], energy-efficient electronic synapses remain a challenge for the neuromorphic engineering community [3–6]. The devices used in this context should be able to emulate physically the biological synapse [7], while also being compatible with CMOS technology, which is an extra requirement. For this purpose and due to their characteristics, two-terminal metal-oxide based RS devices had been proved to be suitable for playing the synaptic role [3–6], where the precise control of the conductance state of the device is an extremely desirable property [7]. RS is often based in the formation (SET process), and partial destruction (RESET process) of a conductive filament (CF) between the two electrodes [7–10]. In this work, the possibility of tuning the conductance state of bipolar RS devices was studied by means of modifying the SET current and the RESET voltage limit during cyclic voltammetry tests.

2. Devices and methods

TiN-Ti-HfO_2-W Metal-Insulator-Metal (MIM) structures with 10 nm oxide thickness and an area of $5 \times 5\ \mu m^2$ (Fig. 1) were tested. HfO_2 was deposited by ALD at 225 °C, with TDMAH and H_2O as precursors. TiN, Ti and W layers were deposited by magnetron sputtering. No postdeposition thermal annealing processes were performed. Two different electrical test schemes were used, involving the smart control of the negative voltage limit (V_{lim}) applied to them, using a software specifically developed for this purpose and a Semiconductor Parameter Analyzer (Ag4156C).

In Figs. 2 and 3, experimental I-V curves of the tested samples are plotted, displaying the typical hysteretic behavior related to the RS phenomena, which in these types of samples is commonly assumed to be controlled by oxygen vacancy transport [10].

The experiment consisted of the application of consecutive, positive and negative voltage ramps in order to induce the SET and RESET

* Corresponding author.
E-mail address: marta.pedro@uab.cat (M. Pedro).

http://dx.doi.org/10.1016/j.mee.2017.04.040
0167-9317/© 2017 Published by Elsevier B.V.

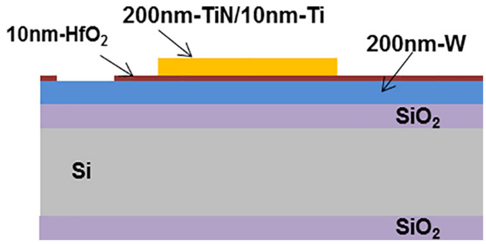

Fig. 1. Schematic of the tested MIM structures.

processes, respectively. For the SET process, the current compliance (I_c) was controlled and varied gradually from cycle to cycle. For the RESET process, two cases were considered: (1) V_{lim} as a fixed voltage, set at $V_{lim} = -1.6$ V (Fig. 2), which is the common procedure, and (2) V_{lim} as the voltage measured when the RESET process was detected as a current drop, and the applied negative voltage ramp was immediately interrupted (Fig. 3). With this latter procedure, the resistance state of the device right after the RESET had occurred could be studied and further compared with the results obtained via the common procedure. The method for the smart control of this interruption consisted of performing a linear fitting of the I-V curve at low voltages during the measurement for each cycle, which was extrapolated at high voltages giving rise to I_{fit}. Values of I_{fit} were then compared to the experimentally measured current values, I_{exp}, and when the ratio of these two parameters was equal or below a certain threshold I_{drop}, the measurement was stopped. In Fig. 3 the current drop detected with this method, as well as I_{fit} and I_{exp} are identified for two different cases. The resistance state of the device after the SET (low resistance state, LRS) and RESET (high resistance state, HRS) was calculated as the V-I ratio measured at |0.2|V.

3. Results and discussion

The LRS and HRS resistances (R) measured for the two testing cases are plotted versus I_c (Fig. 4 top and bottom, respectively). For $I_c >$ 0.1 mA, LRS R decays with increasing I_c [11]. Below this value, no dependence was observed. HRS R values showed no dependence with I_c. For the interrupted measurement, values of HRS R appear much more scattered than for the fixed V_{lim} test configuration.

The result of Fig. 4 shows that the conductance of the device can be tuned at the LRS by applying gradual changes in I_c from cycle to cycle, suggesting the capability of these devices to be used as a synaptic element in neuromorphic circuits. No correlation between I_c and

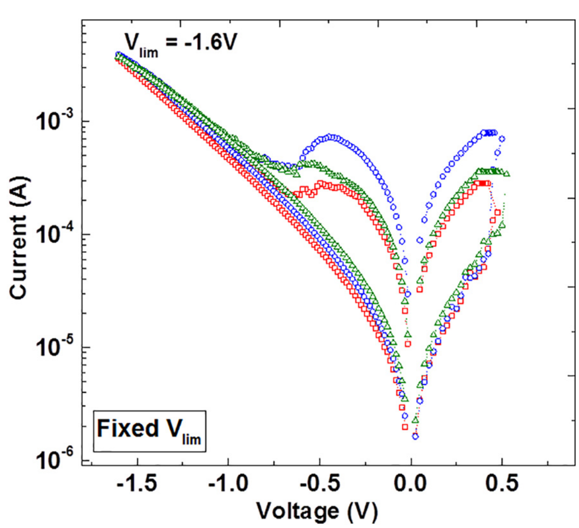

Fig. 2. Example of I-V curves where V_{lim} was fixed to -1.6 V.

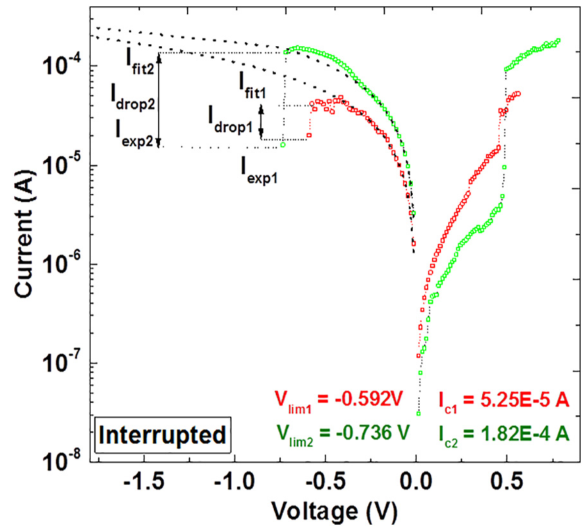

Fig. 3. Example of I-V curves for the interrupted measurement procedure. The dotted line corresponds to the linear fitting of the I-V curve for negative voltages. I_{fit}, I_{exp}, I_{drop}, V_{lim} and I_c for two different curves are indicated.

conductance at HRS is observed, this being caused due to HRS being controlled by V_{lim} [11]. The large variability observed in the interrupted method is attributed to the different V_{lim} values obtained in this case. In Fig. 5, both LRS R values (top) and I_c (bottom) are plotted against the number of cycles, showing that the control of conductance at the LRS is repetitive and also independent of the direction of the change of I_c.

To further investigate the conductivity of the devices, the I-V characteristics at both HRS and LRS for each cycle were fitted to $I = A \cdot V^b$ within the range 0 V–0.2 V. In Figs. 6 and 7, the obtained A/G_o versus *b* coefficients at HRS and LRS are plotted respectively, where A is the conductance (S) of the device if $b = 1$, and G_o is the quantum conductance (77.5 μS) [12–13].

Results displayed in Fig. 6 corresponding to the HRS show that the *b* coefficient is close to 1 for $A/G_o \sim 1$ ($A \sim G_o$). According to the QPC model [12], the CF between the two electrodes is completely formed if $A/G_o \geq 1$,

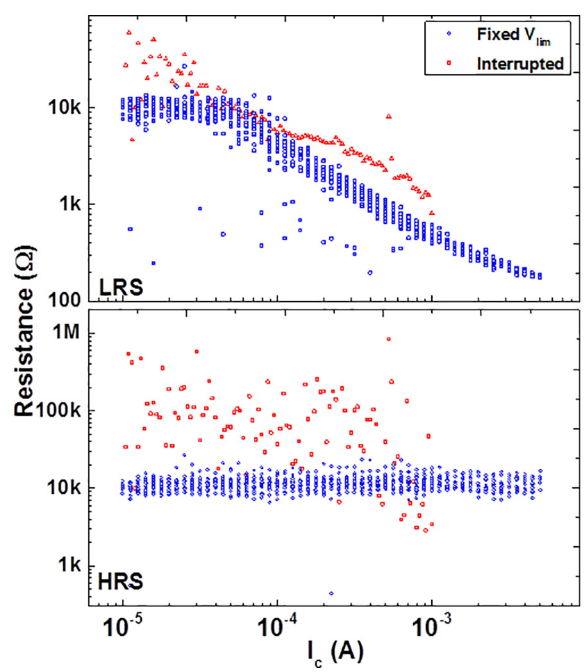

Fig. 4. (Top) LRS and (bottom) HRS resistances measured at -0.2 V, plotted versus the current compliance used for the SET process. Results for the two measurement schemes are shown.